Carbon Nano Tubes Non Equilibrium Electronic Properties And Its Ability In The Future Race Of FET

Yaqubali Mutahhari[1]

Parwan University Afghanistan

ABSTRACT

In this paper we calculate electronic band structure and phonon dispersion of Zig-Zag CNTs. After that we calculate total scattering rate of electron phonon scattering in various CNTs and finally we begin to simulate carrier transport in a Zig-Zag CNT which be used as a channel of FET. We introduce Umklapp Process for Zig-Zag and Armchair CNTs to reduce calculation's.

Keyword: *CNT, CNTFET, Electron Phonon Scattering*

1   Introduction

Indubitably CNTs (Carbon Nano Tubes) will be a good candidate for product new material with new property because of their unique physical and chemical properties. The measured specific tensile strength of a single layer of a multi-walled carbon nanotube can be as high as 100 times that of steel, and the graphene sheet(in-plane) is as stiff as diamond at low strain. These mechanical properties motivate further study of possible applications for lightweight and high strength materials[1]. As we show, one dimensional electronic band structure of CNT's make them as an attractive material for electronic device designs. Many of scientist believe that CNTs can take the Si role in the future of electronic device[2, 3]. The rapid growth of shrinking of transistor make many problem on designing of future race of transistors. As we know a MOSFET (Metal-Oxide-Semiconductor-Field-Effect-Transistor) is made of 5 basic component. 1-Gate, 2-Source, 3-Drain, 4-Gate Oxide, 5-Channel[4]. When a transistor is shrunk all of it's component must be shrunk. When gate oxide be more slim the current tunneling to Gate increase exponentially. Some scientist show Silicon Nitride was a good material instead of silicon oxide because of it's high dielectric constant and it's amorphous structure [5, 6, 7]. Another problem is the length of channel. Making a channel of Si in nano scale is very difficult, because it is very difficult to control the impurity density in nano scale designing. One of solution for this problem is using of CNT's as a channel of FET (Field Effect Transistor) Fig. 1 show a CNTFET structure. We can product pure CNT's in room condition, therefore this material attract many of scientist mind to design future race of CNT's. In this article we study electronic properties of CNT's and simulate carrier transport in Zig-Zag CNT's as a channel of FET.
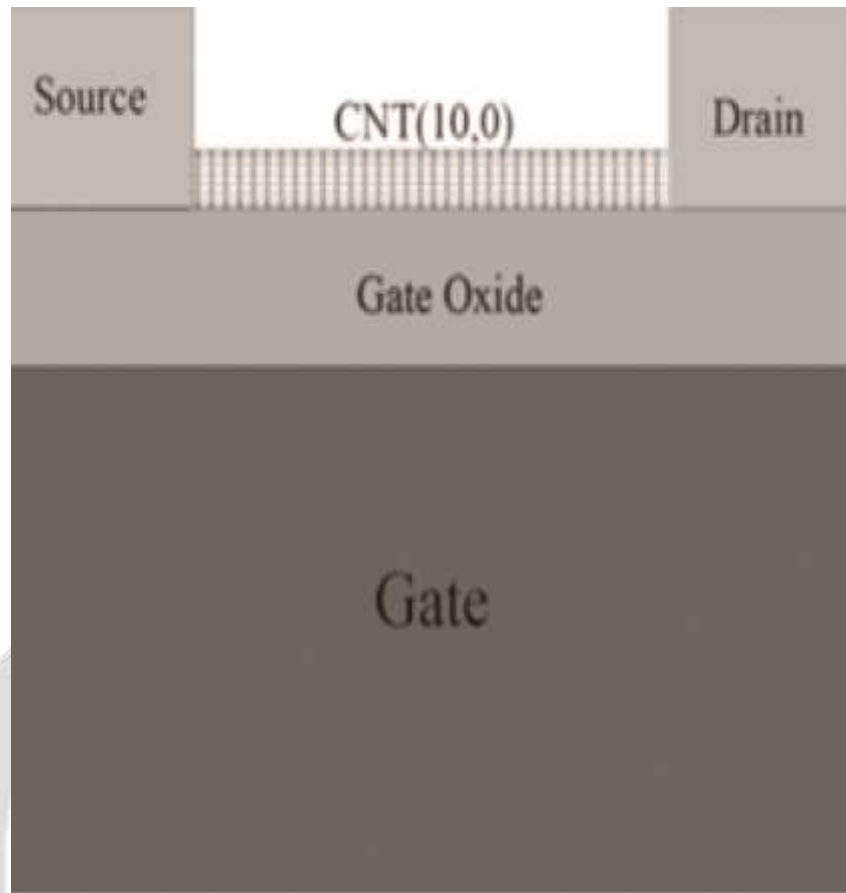
Figure 1: This Figure illustrate a CNTFET structure.

2 SWCNTs Structure

As a theoretical viewpoint SWCNTs(Single Wall Carbon Nano Tubes) can be assumed as a graphene sheet which was rolled into a cylinder[8, 9]. Graphene is also the name commonly associated with a single layer of graphite in two dimensions. The graphene sheet lattice structure is not a Bravais lattice by itself, but can be regarded as an underlying square Bravais lattice with a two - atom basis (called 'a' and 'b') . Graphene is a two dimensional sheet consisting of connected carbon atoms in hexagons like the benzene molecule[10] . The basis of a graphene sheet consists of two atoms named 'a' and 'b', see Fig. 2. When considering only nearest neighbor interaction between e.g. the 'a' atom is connected with three '*b*' atoms, the angle between each 'b' atom is equally spaced with 120° and band length between any carbon-carbon is equal 1.42Å [11]. Because of definition of CNTs their electronic structure can be obtained from those one of graphene sheet. This assumption named Zone-Folding approximation[1].

Graphene sheet consist of 2 atom basis named 'a' and 'b' we can define a Bravais lattice with any 'a' atoms with each other. This lattice define with two basis vector $\vec{a}_1$ and $\vec{a}_2$.

$$\vec{a}_1 = a \left(\frac{\sqrt{3}}{2}, \frac{1}{2} \right) \tag{1}$$

$$\vec{a}_2 = a \left(\frac{\sqrt{3}}{2}, -\frac{1}{2} \right) \tag{2}$$
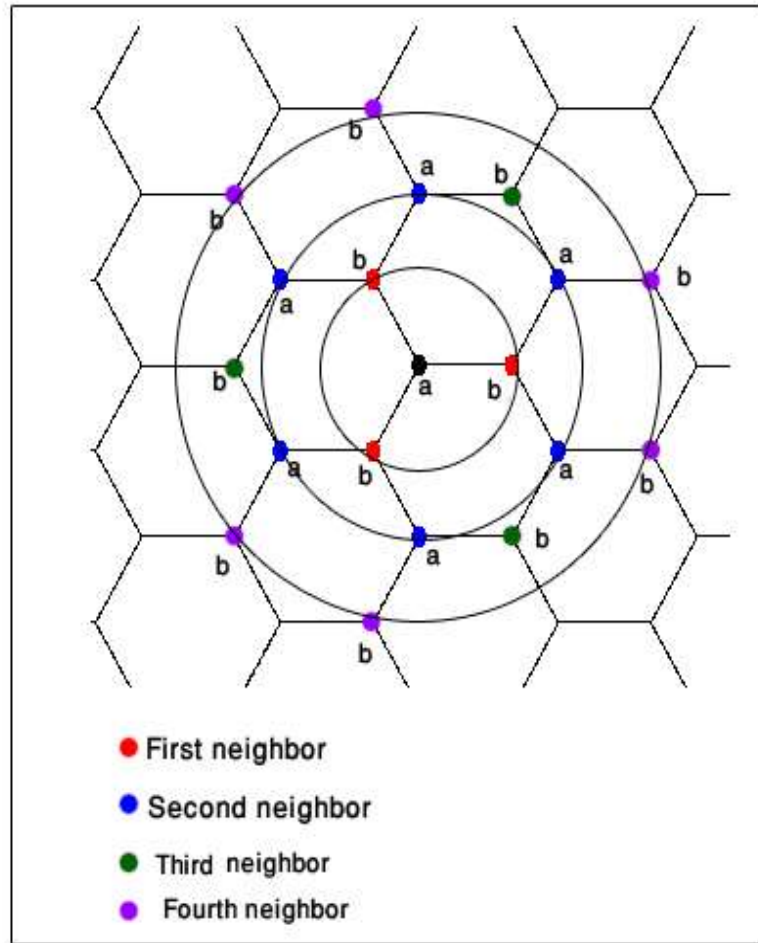
Figure 2:   Graphene structure. this figure show 2 kind of carbon shape in graphene sheet. As you see an 'a' atom has 3 'b' atom in its first neighbor and has 6 'a' atom in it's second neighbor and has 3 'b' atom in it's third neighbor and finally has 6 'b' atom in its 4'th neighbors.

Where *a* is lattice constant of graphene and is equal to 2.46Å[10]. Reciprocal vector of graphene sheet can be obtained with those basis vector of direct lattice[12].

$$\vec{b}_1 = 2\pi \frac{\vec{a}_2 \times \vec{a}_3}{\vec{a}_1 \cdot (\vec{a}_2 \times \vec{a}_3)} \tag{3}$$

$$\vec{b}_2 = 2\pi \frac{\vec{a}_3 \times \vec{a}_1}{\vec{a}_1 \cdot (\vec{a}_2 \times \vec{a}_3)} \tag{4}$$

Where $\vec{a}_3$ is a unit vector perpendicular to the graphene sheet, therefore if we assume geraphene sheet in X-Y plane then $\vec{a}_3 = \hat{z}$

As mention before we can obtained CNT's by rolling graphene sheet into a cylinder. For explain this rolling mathematically you can imagine a cylinder and expand it into a plane. By this work we have a rectangle that it's length is equal to the cylinder circumference and it's width is equal to the cylinder length. So for obtain a CNT from a graphene sheet we must cut a rectangle which it's length be equal to CNT circumference and it's width be equal to CNT height. As you see in Fig. 3 you can find that we can obtain 3 typed CNTs by choosing the form of selection of this rectangle. We want to explain this selection mathematically. The length of this rectangle is called $\vec{C}_h$ and it's name is 'Chiral Vector' [13]. If the angle between $\vec{C}_h$ and X-axis be equal to zero then the CNT which obtain is called Armchair and if this angle was equal to 30° the CNT is called Zig-Zag[1].
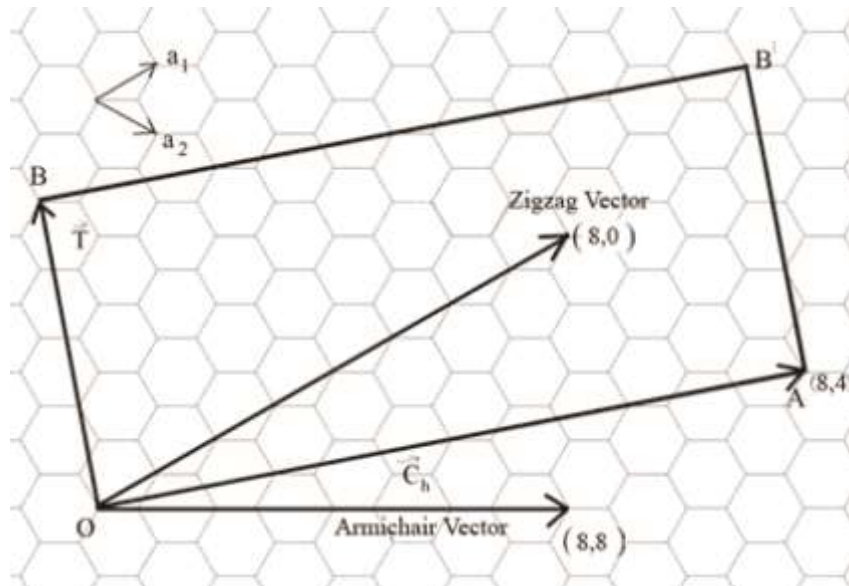
Figure 3: This Figure illustrate a CNT unit cell. In this figure you can realize Zig-Zag vector (8,0) and also armchair vector (8,8) and a chiral vector(8,4) is drown. The rectangle which is made by $\vec{T}$ and $\vec{C}_h$ is the unit cell of CNT (8,4).
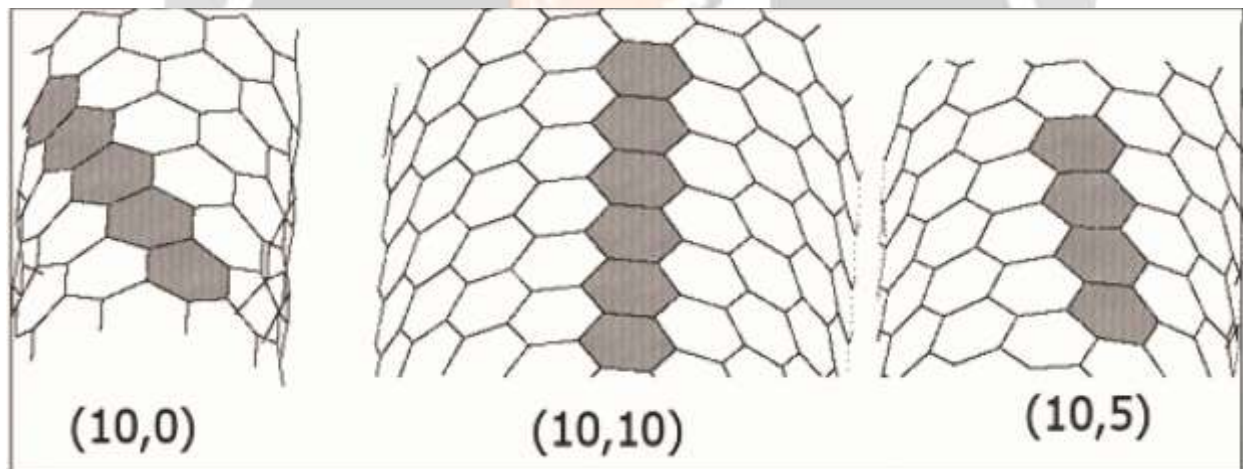
Figure 4: This figure shows 3 kind of CNT's.

By selecting any of angles between [0..30] the CNT is named Chiral. Chiral vector can be expanded by graphene basis vector '$\vec{a}_1$' and '$\vec{a}_2$'.

$$\vec{C}_h = n\vec{a}_1 + m\vec{a}_2 \tag{5}$$

By this definition we can name any CNT associated with its chiral vector by two integer number (n,m). Fig. 4 show 3 kind of CNTs. As mention before the magnitude of chiral vector is equal to circumference of CNT so we can write the radius of CNT as below

$$r = \frac{a\sqrt{n^2+m^2+nm}}{2\pi} \tag{6}$$

Unit cell of CNTs define by a rectangle with a length equal to chiral vector and a width equal to *translation vector*. Translation vector is an smallest vector toward CNT axis which transmit any points to a new points that have same geometrical properties. This vector can be obtained from its definition simply. We can expand translation vector by graphene basis vector '$\vec{a}_1$' and '$\vec{a}_2$'.

$$\vec{T} = t_1\vec{a}_1 + t_2\vec{a}_2 \tag{7}$$

Whereas CNT axis is perpendicular to chiral vector(Chiral vector is perpendicular to the CNT axis) then we can

write

$$\vec{C}_h \cdot \vec{T} = 0 \tag{8}$$

Therefore we can carry out t_1 and t_2 by noting the definition of the translation vector (must be the smallest vector) and by using Eq. 5, 7, 8.

$$t_1 = \frac{n+2m}{GCD(n+2m,m+2n)} \tag{9}$$

$$t_2 = -\frac{2n+m}{GCD(n+2m,m+2n)} \tag{10}$$

Where GCD(a,b) return the Great Common Divisor of integer numbers a and b. As we know from traditional solid state physics[12], the unit cell of graphene, which is made by two basis vector $\vec{a}_1$ and $\vec{a}_2$, is defined by a parallelogram which is made by $\vec{a}_1$ and $\vec{a}_2$ and the unit sell of CNT is defined by a rectangle was made by $\vec{C}_h$ and $\vec{T}$, therefore the number of hexagonal in the unit cell of CNT is then obtained by

$$N = \frac{|\vec{C}_h \times \vec{T}|}{|\vec{a}_1 \times \vec{a}_2|} = \frac{2(n^2+m^2+nm)}{GCD(n+2m,m+2n)} \tag{11}$$

This number is equal to 2n for both Armchair(n,n) and Zig-Zag(n,0) CNTs.

3 Electronic Structure of CNT

Electronic band structure of CNTs is provided from those graphene one (Zone Folding). Electronic band structure of Graphene can be calculated by tight binding theory[14]. Before explain this method for CNTs we first obtain electron wave vector in CNTs.

3.1 Electron Wave Vector of CNT

We now define two wave vector $\vec{K}_\perp$ and $\vec{K}_{||}$, where $\vec{K}_\perp$ is a vector which is parallel to $\vec{C}_h$ and $\vec{K}_{||}$ is a vector that is parallel to the CNT axis and satisfied below condition.

$$\vec{K}_\perp \cdot \vec{C}_h = 2\pi, \quad \vec{T} \cdot \vec{K}_\perp = 0 \tag{12}$$

$$\vec{K}_{||} \cdot \vec{C}_h = 0, \quad \vec{T} \cdot \vec{K}_{||} = 2\pi \tag{13}$$

There are a simple relation between basis vector from direct lattice and those one of reciprocal lattice[12].

$$\vec{a}_i \cdot \vec{b}_j = 2\pi\delta_{ij} \tag{14}$$

From (9), (10), (11), (12), (13) and (14) we can drive $\vec{K}_{||}$ and $\vec{K} \perp$ as below.

$$\vec{K}_\perp = \frac{1}{N}(-t_2\vec{b}_1 + t_1\vec{b}_2), \quad \vec{K}_{||} = \frac{1}{N}(m\vec{b}_1 - n\vec{b}_2) \tag{15}$$

When Graphene sheet is rolled to make a CNT, $\vec{K}_\perp$ is rolled too. So by using periodic boundary conditions in the circumference direction denoted by the chiral vector $\vec{C}_h$, the wave vector associated with the $\vec{C}_h$ direction becomes quantized, while the wave vector associated with the direction of the translational vector $\vec{T}$ (or along the nanotube axis) remains continuous for a nanotube of infinite length. Since $N\vec{K}_\perp$ corresponds to a reciprocal lattice vector , two wave vectors which differ by $N\vec{K}_\perp$ are equivalent. But t_1 and t_2 do not have a common divisor except for unity (as mention before) so there are N discreet value for a wave vector associated with the $\vec{C}_h$ direction. Therefore we can write CNT's wave vector as a continuum component along tube axis and a discrete value of $\vec{K}_\perp$.

$$\vec{K}_\nu^{CNT} = \left(k\frac{\vec{K}_{||}}{|\vec{K}_{||}|} + \nu\vec{K}_\perp\right), \quad \nu = 0\ldots N-1, \quad k = -\frac{\pi}{|\vec{T}|}\ldots\frac{\pi}{|\vec{T}|} \tag{16}$$

We find from this formula that wave vector of a CNT with a given value for ν is a line in direct of $\vec{K}_{||}$. k varies between $-\frac{\pi}{|\vec{T}|}$ to $\frac{\pi}{|\vec{T}|}$ because any one dimensional lattice with a translation vector $\vec{T}$ has a BZ (Brillouin Zone) from that mentioned range[12, 14].

3.2 Graphene band Structure

We obtain graphene band structure by tight binding theory. Any carbon atom is banded to it's three nearest neighbors via sp^2 trigonal very strong single σ bands[15]. The fourth valence (2p) electrons form out-of-plane delocalises π bands, perpendicular to the planes containing the σ bands. While there are strong banded between σ band there not have many role in conduction in graphene. So the main role of conduction is remain for π banding electron[14]. Tight binding model with Bloch wave functions explain a beautiful view of graphene band structure [16]. As we know from traditional solid state, to obtain band structure of a crystal with tight binding model we must solve below equation[16].

$$\sum_i c_i \langle \varphi_j(\vec{r})|\hat{H}|\varphi_i(\vec{r})\rangle = E \sum_i c_i \langle \varphi_j(\vec{r})|\varphi_i(\vec{r})\rangle \tag{17}$$

Where summation is taken over first neighbors and φ is Bloch wave functions and $\hat{H}$ is thigh binding hamiltonian. By sandwiching hamiltonian between two orbital we can obtain banding energy between those orbital. By looking the graphene sheet we find that any 'a' atom is connected with 3 'b' atoms and doesn't have any bonded with 'a' atoms. Therefore the main diagonal element of hamiltonian matrix be equal to zero. The bonding energy of two π orbital is equal to $\beta = -3.03eV$[17, 18]. There are two view point for the overlap integral of two different π orbital. One set it to zero (Slater-Koster scheme). But we don't use this value. In fact the correct value for overlap integral of two different π orbital of carbon in graphene is equal to $s = 0.129$[17, 18]. We can precis the tight binding formula in an algebraic formula as below

$$\hat{H} \cdot C - E\hat{S} \cdot C = 0 \tag{18}$$

This has answer when

$$det(H - ES) = 0 \tag{19}$$

Bloch wave function is defined as below[16].

$$\varphi(\vec{r} + p\vec{R}) = e^{ip\vec{K}\cdot\vec{r}}\varphi(\vec{r}) \tag{20}$$

By noting to geometry of graphene sheet, we find that we must consider three nearest-neighbor 'b' atoms relative to an 'a' atom to extract off diagonal hamiltonian matrix elements. Position of any 'b' atoms is well defined so we can obtain hamiltonian matrix element as below.

$$\hat{H} = \begin{pmatrix} 0 & \beta f(\vec{K}) \\ \beta f^\star(\vec{K}) & 0 \end{pmatrix} \tag{21}$$

$$\hat{S} = \begin{pmatrix} 1 & sf(\vec{K}) \\ sf^\star(\vec{K}) & 1 \end{pmatrix} \tag{22}$$

where $f(\vec{K})$ is a function of wave vector $\vec{K}$ and is equal to

$$f(\vec{K}) = \sqrt{1 + 4cos\left(\frac{\sqrt{3}K_x a}{2}\right)cos\left(\frac{K_y a}{2}\right) + 4cos^2\left(\frac{K_y a}{2}\right)} \tag{23}$$

By solving Eq. 19 we can obtain graphene band structure.

$$E = \frac{\pm\beta|f(\vec{K})|}{1 \pm s|f(\vec{K})|} \tag{24}$$

Where '+' refer to π bonding and '-' refer to $\pi^\star$ bonding and a is lattice constant of graphene. Fig. 5 show the graphene band structure. As you see in this figure graphene has 2 band level. One with negative energy denote valance band other with positive energy denote conduction band. As you see in this figure valence band is touch conduction band in 6 points. Graphene is a quasi metal because it has 2d band structure (is dependent only with K_x and K_y) but it's valence band and conduction band touch each other only in some points.
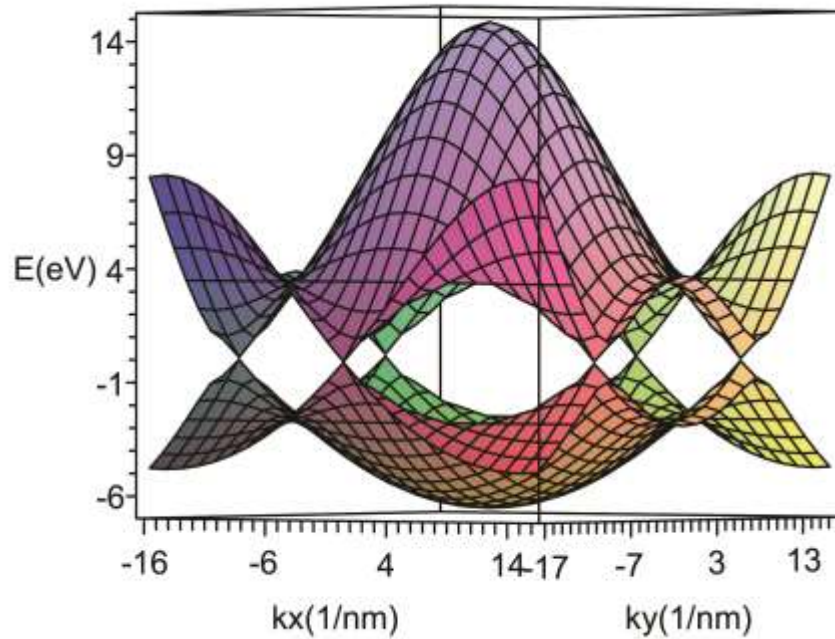
Figure   5:   Graphene band structure. As you see the conduction band touch valence band in 6 points.

3.3   CNT band Structure

According to the definition of SWCNT, the energy bands of a SWCNT consist of a set of one-dimensional energy dispersion relations which are cross sections of those of graphene. By using Eq. 16 and put it in Eq. 24 we can drive SWCNT band structure. Fig. 6 show some band structure of CNT's.
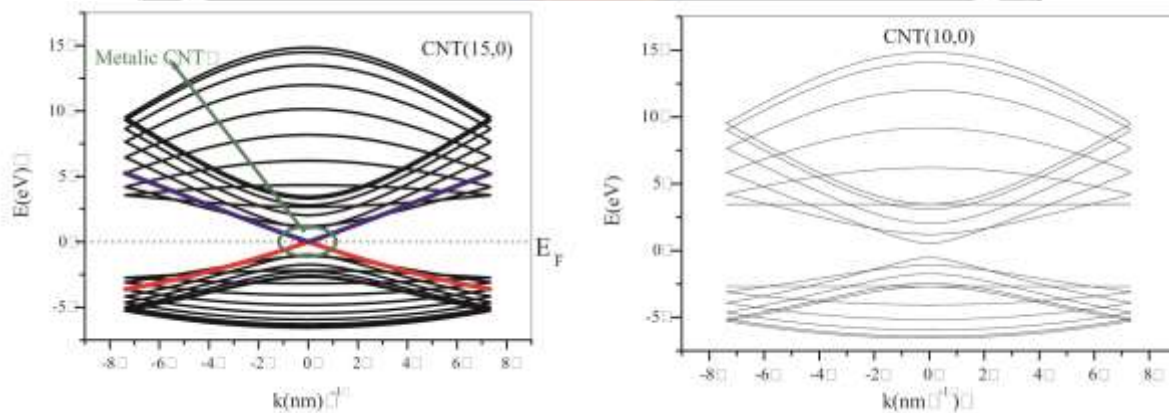

Figure   6:   Electronic band structure of some CNTs based on Tight-binding model. The banding energy of π orbital is equal to -3.03 eV and its overlap matrix is equal to 0.129. This figure clearly show that CNT (15,0) is a metallic CNT. We will drive an important relation between the geometry of CNT and it's conduction. There are an important note. *There are $\frac{N}{2} + 1$ degenerate levels in Zig-Zag CNT(n,0) . Therefore CNT(10,0) 11 realizable energy level. This is happened for armchair CNTs too*
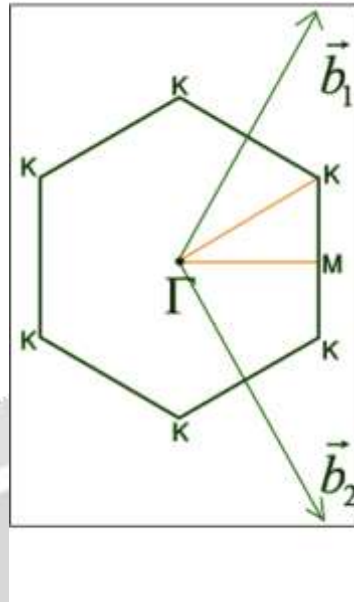
Figure   7:   This Figure illustrate first Brillouin Zone of graphene .

Now we extract an important relation between geometric parameter of CNT's and it's electronic conduction. As we see in Fig. 5 band levels of graphene is touch each other in 6 points. This points is one of 3 high symmetry points in graphene first BZ. First BZ of graphene is shown in Fig. 7 and 3 high symmetry points is labeled as Γ and K and M. band levels of graphene meet each other at 6 K points. The symmetry of band levels of graphene due to first BZ, make this 6 points to have a similar treatment. So considering any property of one of this 6 points is equivalent to each 5 other. The position of one of K points in the first BZ of graphene is equal to $\left(\frac{2\pi}{\sqrt{3}a}, \frac{2\pi}{3a}\right)$ [14]. So if any of the band level of CNT transits from this point the CNT treat as a conductor. But if there are not any transits from this point CNT treat as a semiconductor. As we see in Fig.8 the band gap of CNT's in semiconducting shape is start from near 1 for SWCNT's with little radius (10,0) and decrease by increasing on the radius. Therefore CNT's which it's radius is larger than CNT(10,0) is treat as semiconductor.
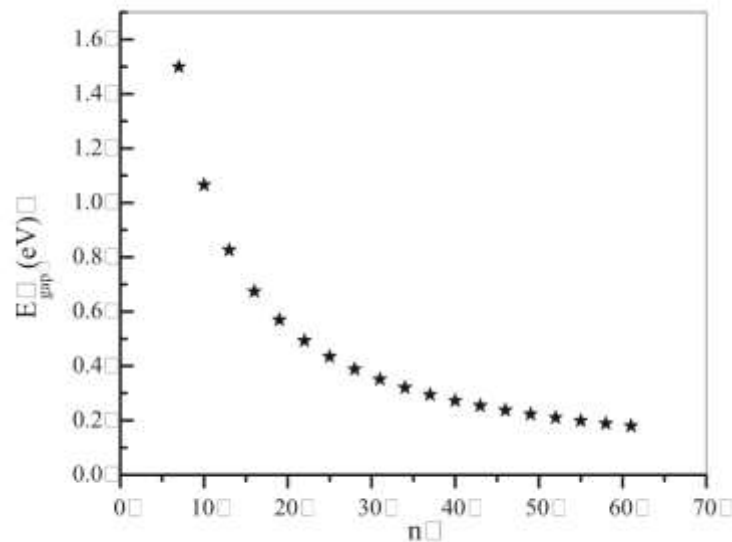
Figure   8:   This Figure show band gap of semiconducting Zig - Zag (n,0) CNTs. As you see the band gap decay by increment on CNT radios.

We can write

$$\vec{K}_v^{CNT} \cdot \vec{C}_h = 2\pi v \tag{25}$$

and chiral vector is define as below

$$\vec{C}_h = \left(\frac{(n+m)\sqrt{3}}{2}, \frac{n-m}{2}\right) \tag{26}$$

Since the wave vector of CNT with a given value for v is a line so if one band level of CNT want to cut Point K then the coordinate of this point must satisfied Eq. 25. By putting $\left(\frac{2\pi}{\sqrt{3}a}, \frac{2\pi}{3a}\right)$ instead K_v^{CNT} and put Eq. 26 in Eq. 25 we obtain an important condition for conducting CNT's

$$\frac{2n+m}{3} = v \tag{27}$$

This relation said to us, if (2n+m) or in the other word if (n-m) be a multiple of 3 then the CNT is a conductor. Density of State of a one dimensional lattice with a lattice vector $\vec{T}$ and for one level is given by [16]

$$g_i(\varepsilon) = \frac{|\vec{T}|}{\pi} \frac{1}{\left|\frac{\partial E_i}{\partial k}\right|_{E_i=\varepsilon}} \tag{28}$$

$$DOS(\varepsilon) = \sum_i g_i(\varepsilon) \tag{29}$$

Fig. 9 Show DOS of some CNT's. As we see in this figure semiconducting Zig-Zag CNT's have not any density of state at the Fermi level but armchair CNT's have a little density of state at Fermi level. If we focused to the armchair CNTs in around fermi level we find that the DOS has not treat as a constant value and treat as a parabola curvature (Some workers show that Armchair CNTs have a constant DOS around Fermi level[19] , but it isn't. This is important in some case that the differential of DOS is appeared).
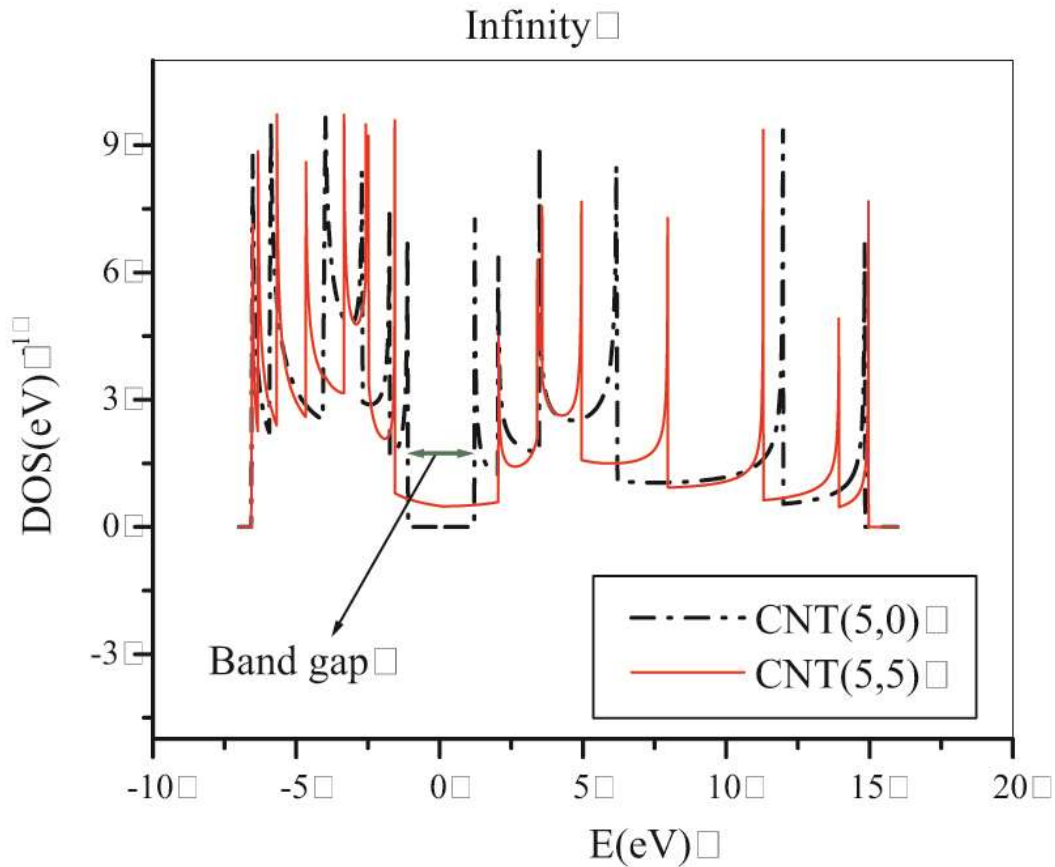
Figure 9:   This figure compares density of state of a Zig-Zag CNT via as an armchair CNT. As you see the Zig-Zag CNT has not any DOS near the fermi level.

4   Phonon dispersion Of CNT

The phonon dispersion relations of SWCNTs can be calculated using zone folding [20], tight-binding methods[21, 22, 23, 24], density functional theory [25, 26], and symmetry-adapted models [27, 28]. The phonon dispersion relations of SWCNTs can be understood by zone folding of the phonon dispersion branches of graphene. In this work we have calculated phonon dispersion of a graphen sheet by force constant model. In this model we have applied the effect of 4 nearest neighbors. Since there are two carbon atoms, in the unit cell of graphene, one must consider 6 coordinates. The secular equation to be solved is thus a dynamical matrix of rank 6, such that 6 phonon branches are achieved. In order to determine phonon dispersion relation we consider the sum of the forces on the ith atom, $\vec{F}_i$, for N atoms in the unit cell as follow (there are 2 atoms in the unit cell of graphene).

$$\vec{F}^i = \sum_j K^{ij}\big(\vec{u}_j(\vec{R}_j) - \vec{u}_i(\vec{R}_i)\big) \tag{30}$$

Where $\vec{u}_i$ is the displacement of the ith atom and K^{ij} is a 3×3 force constant matrix between the ith and the jth atom. $\vec{R}_i$ denotes the original position of the ith atom. The sum over j in Eq. 30 is normally taken over only a few neighbor distances relative to the ith site, which for a 2D graphene sheet has been carried out up to 4th nearest-neighbor interactions [21]. The equation of motion is given by below equation

$$M\ddot{\vec{u}}_i = \vec{F}_i \tag{31}$$

Where M is the mass of the carbon and is equal to $2 \times 10^{-26} kg$. In a periodic system we can perform a Fourier transform of the displacement of the ith atom to obtain the normal mode displacements u_i. Before note that we label Phonon wave vector with $\vec{Q}$ to realize that form electron one in our calculations. When we assume the same eigenfrequencies ω for all $\vec{u}_i$, (only for low temperature this assumption is correct we do some calculation for nonlinear term in Phonon dispersion in [29]), then from fourier translation we can write below expression for $\vec{u}_i(\vec{R})$

$$\vec{u}_i(\vec{R}) = \frac{1}{\sqrt{c}} \Sigma_{\vec{Q}'} \, e^{-i(\vec{Q}' \cdot \vec{R}_i - \omega t)} \vec{u}_{\vec{Q}'}^i \tag{32}$$

By taking differential form this equation twice and put it in Eq. 31 we obtain below equation for motion

$$\left(\Sigma_j \, K^{ij} - \omega^2 M_i \hat{I}\right) \frac{1}{\sqrt{c}} \Sigma_{\vec{Q}} \, e^{-i(\vec{Q} \cdot \vec{R}_i - \omega t)} \vec{u}_i(\vec{Q}) = \Sigma_j \, K^{ij} \frac{1}{\sqrt{c}} \Sigma_{\vec{Q}} \, e^{-i(\vec{Q} \cdot \vec{R}_j - \omega t)} \vec{u}_j(\vec{Q}) \tag{33}$$

With multiply two side of this equation by $e^{i\overrightarrow{Q'} \cdot \vec{R}_i}$ and summation over all $\vec{R}_i$ and nothing that

$$\Sigma_{\vec{R}_i} \, e^{i(\vec{Q} - \overrightarrow{Q'}) \cdot \vec{R}_i} = \delta_{\overrightarrow{QQ'}}$$

Eq. 33 take simple form as below

$$\left(\Sigma_j \, K^{ij} - \omega^2 M_i \hat{I}\right) \vec{u}_i(\vec{Q}) - \Sigma_j \, K^{ij} e^{i\overrightarrow{Q\Delta R}_{ij}} \vec{u}_j(\vec{Q}) = 0 \tag{34}$$

Where $\Delta \vec{R}_{ij} = \vec{R}_i - \vec{R}_j$. Eq. 34 can be written as a secular matrix shape as below

$$D(\vec{Q}) u(\vec{Q}) = 0 \tag{35}$$

Where dynamical matrix D is a $3N \times 3N$ (for graphene 6×6) matrix. It is convenient to divide the dynamical matrix $D(\vec{Q})$ into small 3×3 matrices D^{ij} as below .

$$D = \begin{pmatrix} D^{aa} & D^{ab} \\ D^{ba} & D^{bb} \end{pmatrix} \tag{36}$$

Where D^{ij} is defined respect to equation of motion and Fourier transform as below

$$D^{ij}(\vec{Q}) = \Sigma_{j\dagger} \, (K^{ij\dagger} - M\omega^2)\delta_{ij} - \Sigma_{j'} \, K^{ij'} e^{i\vec{Q} \cdot \Delta \vec{R}_{ij'}} \tag{37}$$

Where summation over j' is taken over the 4th near neighbors and summation over $j^\dagger$ is taken over the neighbors of 4th atom respect to i'th atom which be equal to the j' type atom. So we can obtain any element of this matrix as below(see Fig. 2)

$$D_{aa} = K^{ab_1} + \ldots + K^{ab_{12}} + K^{aa_1} + \ldots + K^{aa_6} - K^{aa_1} e^{i\vec{Q} \cdot \Delta \vec{R}_{aa_1}} - \ldots - K^{aa_1} e^{i\vec{Q} \cdot \Delta \vec{R}_{aa_6}} \tag{38}$$

$$D_{ab} = -K^{ab_1} e^{i\vec{Q} \cdot \Delta \vec{R}_{ab_1}} - \ldots - K^{ab_{12}} e^{i\vec{Q} \cdot \Delta \vec{R}_{ab_{12}}} \tag{39}$$

To obtain the eigenvalues for D and non-trivial eigenvectors $u_Q \neq 0$, we solve the secular equation $det D(\vec{k}) = 0$ for a given $\vec{Q}$ vector. Force constant matrix K^{ij} was explained respect to 4th nearest neighbors in deferent references [21, 30, 31]. You can obtain this element theoretically by using well known carbon-carbon potential like as Tersof-Berner, Morse potential and harmonic potential[32, 33, 34] and applying a little displacement to any carbon atom to drive forces. When forces is obtained you can drive Force Constant Matrix element. We use this method not for obtaining matrix element but for obtain nonlinear effect of vibration[29]. The work which obtain this elements is a beautiful work to compare experimental results with those theory one. We solve $det D(\vec{Q}) = 0$ and drive phonon dispersion for graphene. Fig. 8 shows phonon dispersion of geraphen. Because the unit cell of graphene is equal to two atoms and any atoms have 3 freedom of degrees so we expect, we obtain 6 branches of phonon for graphene. 3 of them be acoustic phonon which its energy is *increase* by an *increment* to the magnitude of wave vector of phonon and 3 optical phonon which it's energy is *decrease* by an *increment* to the magnitude of wave vector. By solving 6×6 secular determinant of dynamical matrix we obtain 6 branches of phonon dispersion as be illustrated in Fig. 10.
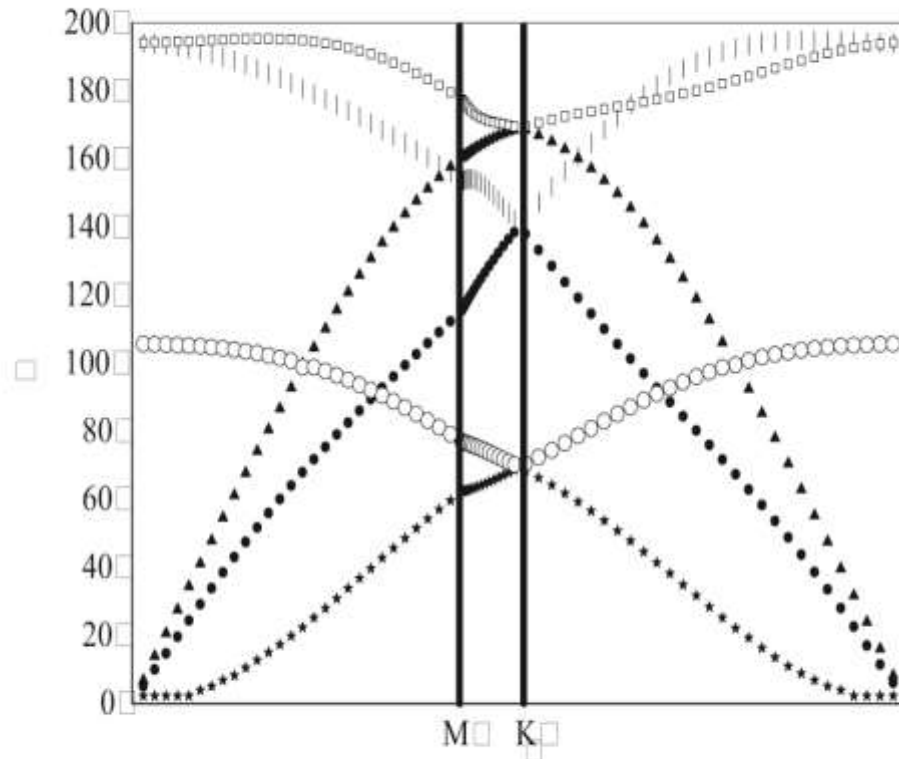
Figure   10:   Phonon dispersion of graphene along high symmetry points.

The phonon dispersion relations for a SWCNT can be determined by folding that of a graphene layer as we done before for band structure of SWCNT . The corresponding one-dimensional phonon energy dispersion relation for the CNT is given by

$$\hbar\omega_\nu^{CNT}(q) = \hbar\omega^{Graph}(q\frac{\vec{Q}_\perp}{|\vec{Q}_\perp|} + \mu\vec{Q}_{||})$$
                                                                                            (40)

 Since there are 6 branches of phonon dispersion and each branches take N value for $\mu = 0\dots N-1$ so there are 6N branches for phonon dispersion relation. For example in the CNT(10,0) we obtain N=20 and so there must be 120 phonon dispersion relation but as mention before (Fig. 6) Zig-Zag CNTs and Armchair CNTs band structure have $\frac{N}{2}+1$ degenerate level so we have only 11 distinguishable level for CNT(10,0) and so there are 66 distinguishable level for Phonon branches of this CNT (Fig. 11)
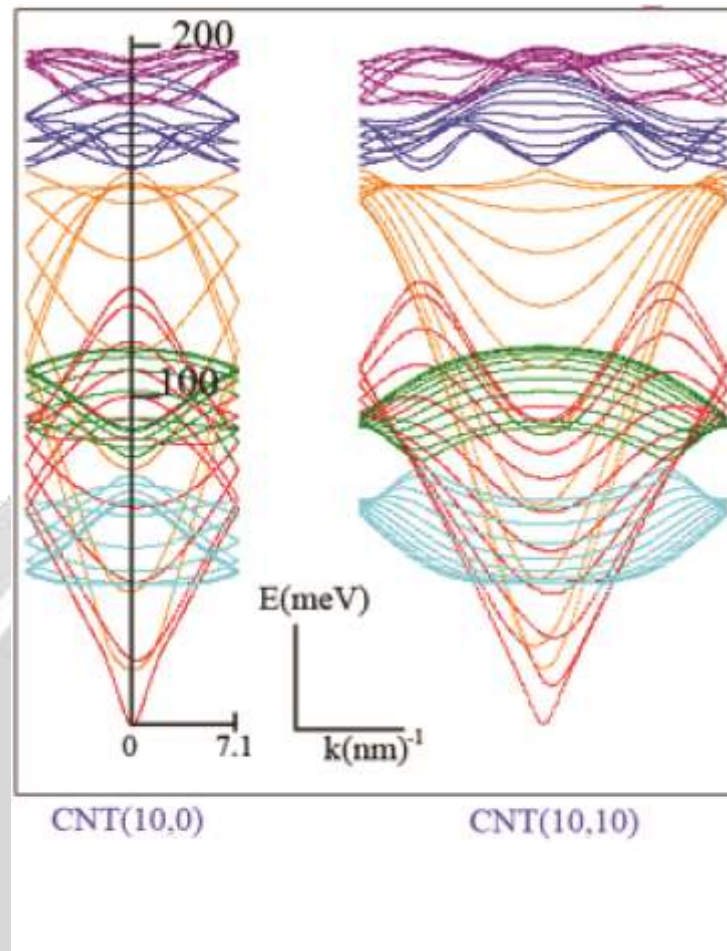
Figure 11: Phonon dispersion of CNT(10,0) and CNT(10,10).

5 Electron-Phonon Scattering in CNT's

While the effects of scatters such as lattice defects can be potentially reduced in synthesis, phonon scattering is intrinsic to the nanotube and determines the performance limits of the device. Now we want show the application of the last section in an application work. As mention before the idea where use a SWCNT instead of Si channel in a FET is formed in the recent years. We now simulate carrier transport in a CNTFET by using Monte Carlo method for selecting scattering mechanism and taking an average to the carrier velocity by obtaining their distribution function on a presence of electric field and scattering mechanism. As we know from traditional solid state[16, 35, 36] the initial distribution function was deformed in an existence of fields and scattering phenomena. Because carrier in CNTFET can be boat electron (by applying a positive voltage to gate) or the hole one (by applying a negative voltage to gate) [15] the initial distribution function that describe them is Fermi-Dirac distribution function. Imagine a Zig-Zag CNT which is a semiconductor . If we use it as a channel of FET and apply a potential to the gate then some charges was sprayed to the CNT. This charges treat as impurities role in natural semiconductors and change fermi level toward conduction band (electron transportion) or toward valence band(hole transportion). The charge is sprayed because the gate and the gate-oxide and CNT make a capacitor with a capacitance of[37, 38].

$$C = \frac{2\pi\kappa\varepsilon_0 L}{ln\left(\frac{2(t+r)}{r}\right)} \tag{41}$$

Where r is tube's radius and t is the thickness of the gate oxide and L is the CNT length. Using Fermi's golden rule, the phonon mediated scattering rate from initial carrier state k to final carrier state k' is given by [39, 40]

$$W_{\vec{k},\vec{k}'} = \frac{D^2 DOS(\overrightarrow{k'})}{\rho d\omega_p}\left(N_p + \frac{1}{2} \pm \frac{1}{2}\right) \tag{42}$$

Where N_p is Bose - Einstein occupation number and ρ is mass density of graphene sheet and D is deformation potential and be equal to

$$D = D_0\left(\frac{2}{d}\frac{E_p^2(q=0)}{E_{RBM}^2} + q\right) \tag{43}$$

where $D_0 = 14eV$ and $E_{RBM} \approx \frac{28meV}{diameter of CNT}$ and q is phonon wave vector and E_p is phonon energy. For the determination of electron-phonon scattering rates electron band structure and phonon dispersion is divided into 2000 grid points covering first BZ . The requirements of energy and momentum conservation lead to following selection rules for final electron state.

$$E_f = E_i + E_{ph} \tag{44}$$

$$\vec{k}_f = \vec{k}_i \pm \vec{q} \tag{45}$$

where $\vec{k}$ refer to electron and $\vec{q}$ refer to phonon wave vector. Based on final state of electron after scattering, two different processes are possible. They are Normal process and **Umklapp** process. A Normal process results in a final electron wave vector $\vec{k}_f$ that lies within the first BZ, while an Umklapp process results in a $\vec{k}_f$ that lies outside first BZ,a reciprocal lattice vector needs to be added to it to transmit it to the firs BZ. We can define a procedure respect to symmetry of Zig-Zag and Armchair CNTs, that give an equivalent point in the first BZ. In case of Zig-Zag or Armchair CNTs, any point out of First BZ can translate to first BZ by below translation formulism.

$$k'_f = \frac{2\pi}{T} + k_f, \quad v'_f = \begin{cases} n - v_f & 0 \le v_f \le n \\ v_f - n & v_f > n \end{cases} \quad if \ k_f < -\frac{\pi}{T}$$

$$k'_f = -\frac{2\pi}{T} + k_f, \quad v'_f = \begin{cases} n - v_f & 0 \le v_f \le n \\ v_f - n & v_f > n \end{cases} \quad if \ k_f > \frac{\pi}{T} \tag{46}$$

$$k'_f = k_f, \quad v'_f = 2n - v_f \ if \ v_f > n \quad and \quad |k_f| \le \frac{\pi}{T}$$

Total scattering rate is define as summation over all final state, k'.

$$W_{Total}(\vec{k}) = \sum_{\overrightarrow{k'}} W_{\vec{k},\overrightarrow{k'}} \tag{47}$$

and relaxation time, $\tau(\vec{k})$, is defile as below[41, 42].

$$\tau(\vec{k}) = \frac{1}{W_{Total}(\vec{k})} \tag{48}$$

The distribution function of electron or hole can be varied by applied electric or magnetic fields and scattering phenomena. We have investigated carrier transport in single-walled semiconducting carbon nanotubes by solving the Boltzmann equation.

$$\frac{\partial g_n(\vec{r},\vec{k},t)}{\partial t} + \vec{v}.\vec{\nabla}_r g_n(\vec{r},\vec{k},t) + \vec{F}.\vec{\nabla}_k g_n(\vec{r},\vec{k},t) =$$

$$\sum_{k'}\left[W_{\vec{k},\vec{k'}}g_n(\vec{r},\vec{k},t)(1 - g_n(\vec{r},\overrightarrow{k'},t)) - W_{\overrightarrow{k'},\vec{k}}g_n(\vec{r},\overrightarrow{k'},t)(1 - g_n(\vec{r},\vec{k},t))\right] \tag{49}$$

It is now possible to simplify Eq. 49 by using relaxation time approximation[16].

$$\frac{\partial g_n(\vec{r},\vec{k},t)}{\partial t} + \vec{v}.\vec{\nabla}_r g_n(\vec{r},\vec{k},t) + \vec{F}.\vec{\nabla}_k g_n(\vec{r},\vec{k},t) = -\frac{g_n(\vec{r},\vec{k},t) - g_n^0(\vec{r},\vec{k},t)}{\tau} \tag{50}$$

Where g_n^0 is initial distribution function of nth branch of energy dispersion of CNT which is independent on scattering phenomena and applied field. We have assume a Fermi - Dirac distribution function for unaffected electron. So if CNT Length be assumed very large we can neglect derivation due to position vector.

$$g_{n,el}^0(k,t) = f_{n,el}^0(k) = \frac{1}{e^{\frac{E_n(\vec{k})-\mu}{K_B T}}+1} \tag{51}$$

$$g_{n,hole}^0(k,t) = 1 - f_{n,el}^0(k) \tag{52}$$

Where $E_n(\vec{k})$ is electron energy and the wave function of electron is assumed as a Block function. The velocity of electrons can be obtained from semiclassical motion relation as below[16].

$$V_n(\vec{k}(t)) = \frac{1}{\hbar}\vec{\nabla}_k E_n(\vec{k}, t) \tag{53}$$

Fermi level can be obtained from below relation.

$$n = \int f(k)dk \tag{54}$$

n is electron (hole) density. When we applied a voltage to gate some charges are sprayed to CNT and we can find electron density simply by dividing the number of this charges to CNT length. f(k) is those Fermi - Dirac function. We show Fermi level for a wide range of CNTs in Fig. 12. As you see in this picture the fermi level decay by increment on CNT radios.
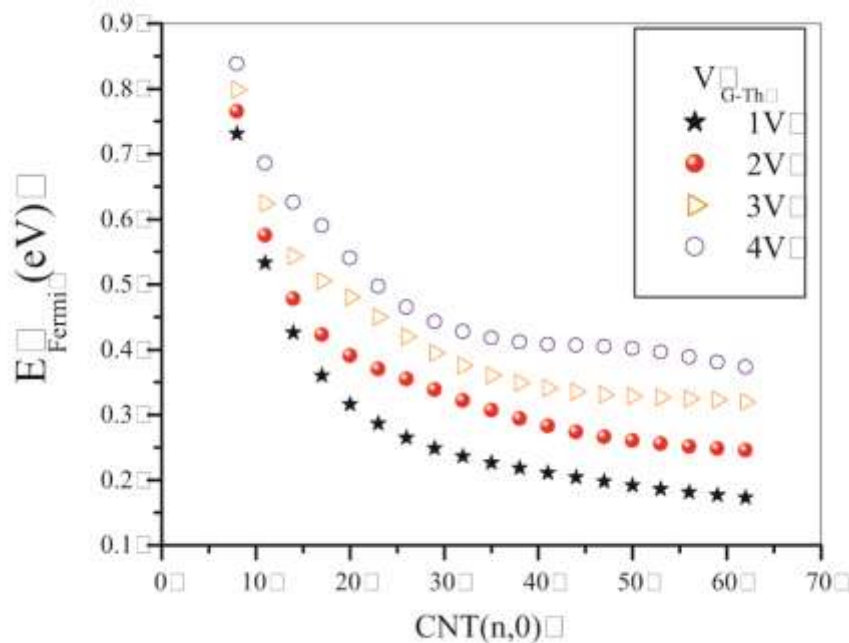
Figure 12: This picture shows how fermi level decay by increment of n.

The average of velocity is obtained as below.

$$\bar{V} = \left(\sum_i V_i g_n(k_i, t_i)\right) \times \left(\sum_i g_n(k_i, t_i)\right)^{-1} \tag{55}$$

$$and \quad t_i = it_d$$

As we know the carrier density is an integral over distribution function[35, 16]. So we can write

$$n(t) = \sum_v \int_{-\frac{\pi}{T}}^{\frac{\pi}{T}} g_v(k, t)dk \tag{56}$$

and

$$\bar{n} = \frac{1}{t}\int_0^t n(t')dt' \tag{57}$$

In this simulation we let carrier scatter in a time around 10000 times of the maximum of relaxation time. When carrier drift for a drift time we calculate the total time of the carrier that has not any scattering before it. Now we generate a random number and compare it to the ratio of this time to drift time. If the random number is smaller than this ratio we must select a random scattering mechanism. We know that the current is made by charge moment. Therefore if we multiply the average charge density to the average velocity we cane drive the average current.

$$I_{DS} = |\bar{n}e\bar{v}| \tag{58}$$
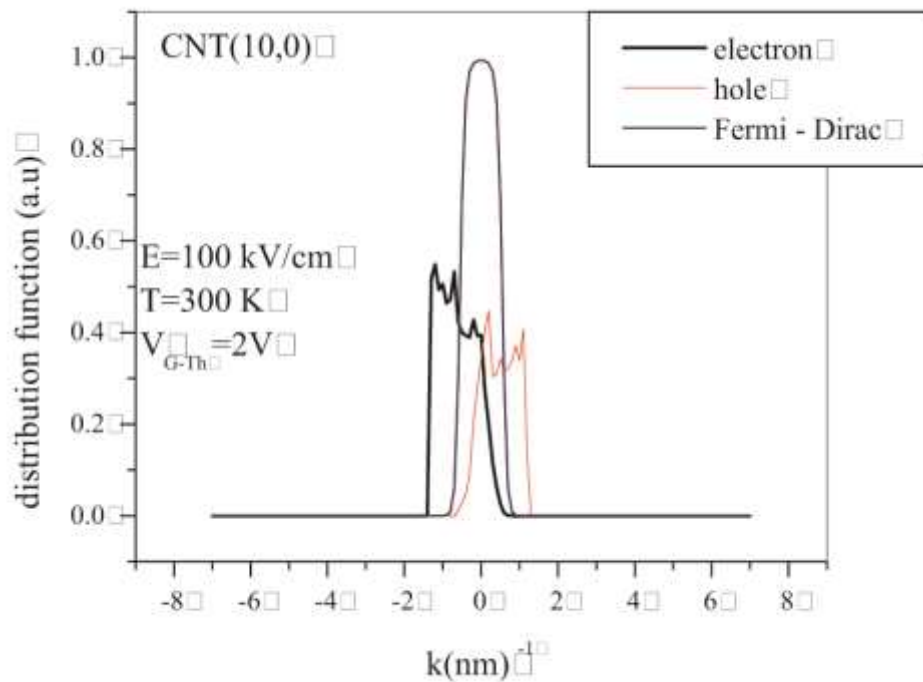
Figure 13: Distribution function of CNT(10,0) for electron and hole. As you see wen we apply an electric field along tube axis the electron distribution be shifted to the left side while the hole one shifted to the right side. This causes electrons and holes take an acceleration from field in a common direction, because the velocity of conduction band in the left side is negative and it is negative for valence band in the right side too (see Eq. 52 and Fig. 6)
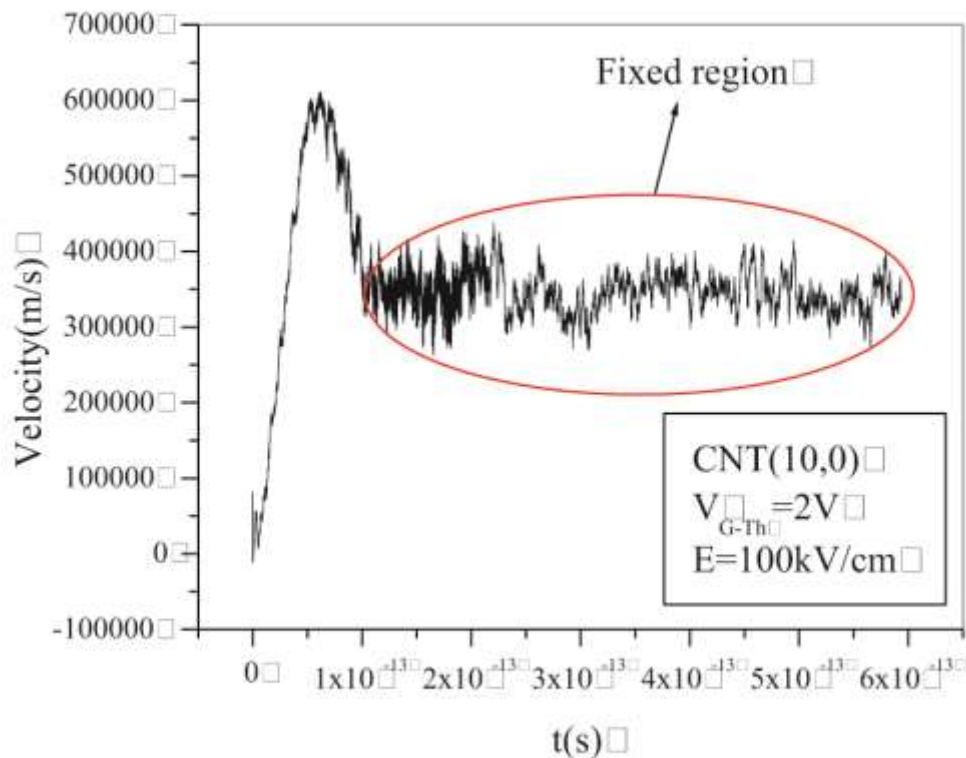
Fig.13 shows distribution function of electron in lowest conduction band versus the hole one in the maximum of valence band. By noting at Fig.6 we find that the direction (sign) of velocity for a given wave vector in maximum of valence band correspondent to it's in minimum of conduction band, is opposite to each other. On the other hand distribution function of holes and electrons was shifted opposite to each other around k=0. So by applying an electric field along the tube axes the absolute current of carriers was happened towards against the field directions *(this means the current of electrons and holes in an electric filed was happened in a same direction)*. We completely know that Fermi-Dirac distribution function change very sharp around fermi level. So it's differential has a magnitude only around fermi level. Therefore scattering to the level that is far from fermi level has not any contribution in averaging for velocity. This means for CNTs with little radius which fermi level is only close or cut firs level band the other level has not any contribution in the velocity. But as we sea in Fig.8 by increasing in radius of CNT band gap was decreased. On the other hand the compactness of energy levels was increased. This means for CNT's by larger radius fermi level can cut more than one band level and averaging for velocity contain the contribution of this level so there are complicated relation on the dependent of carrier velocity and the tube radius . Only the stimulation results can explain this dependent for us.

5.1 Result Of Simulation

The simulation results show that when the system spend a time more than $10^{-13}s$ the distribution function take a uniform shape, this means *by spending this time the system is transferred to an stationary condition*, Fig.14 show the time dependent of electron velocity. As you see the velocity take a uniform value for a time bigger than $2 \times 10^{-13}s$. We have simulated a CNTFET with a gate oxide by 10nm thickness and a channel which made by a CNT(10,0) with a length of 100nm. The average velocity is shown in Fig.14. As you see for a defined region of voltage the velocity of electrons treat as a linear shape and take a uniform shape for a potential bigger than this voltage. One of the most important factor of FETs is the speed of switching between on-off states. So the the velocity - voltage curvature of a

CNTFET must have an acceptable slope, therefore the best range of potential of a CNTFET is those range that the velocity - voltage curvature has a linear shape.
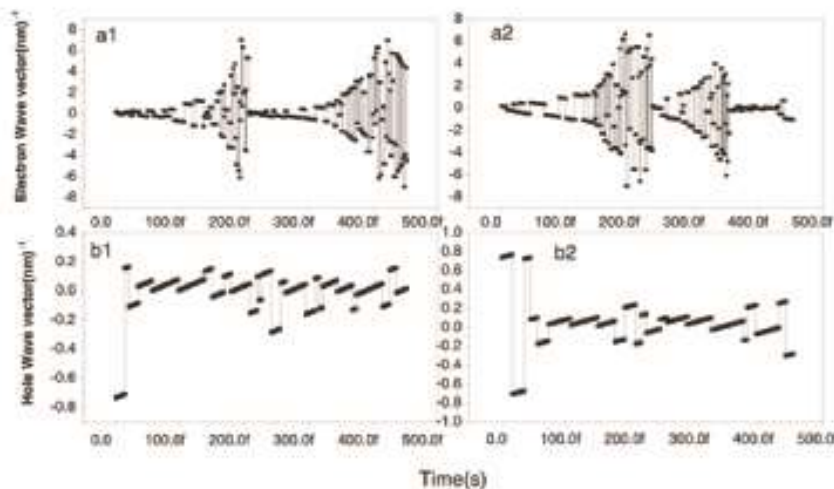

Figure 14: This figure show that how an electron take accelerate in the field by passing time. The velocity take a maximum value and then tend to a constant value. As mention before this cause by the stable condition for distribution function after a time around $10^{-13}s$

Fig.15 show the major importance between electron transport and the hole one. As you see the hole transport make an small. In both (electron - hole) the velocity take a uniform shape per strong field. This means the CNTFET which is made by a CNT(10,0) can not work on high electric field if we expect of this transistor in switching device like CPU memory or computer memory. In this case the most factor which is important for us is the ability of anticlimax (on -off) of transistor. So the slope of velocity - field is more important factor for us in designing a CNTFET . Fig. 16 show that CNT (10,0) has an acceptable slope in its velocity - field curvature in the range of (0.5 - 3 MV/m). As you see in Fig.6 the velocity of valence band, which obtain from the gradient of energy respect to wave vector, is litter than concoction one. Therefore it is clearly that the average of hole velocity be smaller than electron. Fig.16 and Fig.17 show another differences between electron transport and the hole one. As you see in this figures the electrons are scattered to total energy level but holes scattered only in the maximum level of valence band. Note that the initial state of holes is in the maximum level of valence band and they stay in this level forever. Other deference between hole scattering and electron scattering is the amount of scattering. Electrons scatters more than holes and take a wide range of wave vectors but the hole ones stay only in an small range of wave vector. Fig.18 show the average of electron density in the CNT(10,0). This figure show electron density decays with increment of the electric field along the tube axis. Fig.19 show the current of electron transport in a CNTFET by using a CNT(10,0) as it's channel.
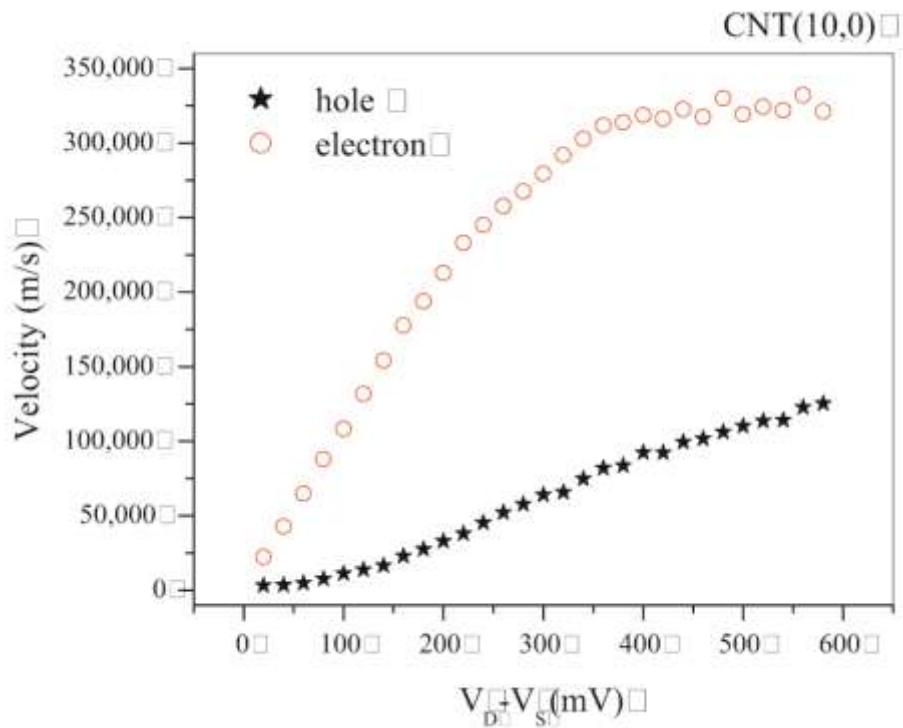
Figure 15: his figure compare electron transport versus as hole one. As you see electrons take more velocity from filed, Consequently, the current which obtain from electron transport is more than hole one.

Figure 16: This figure compare electron scattering versus as hole one. This figure show that electrons scattered in many level of energy but the hole one stay only in the maximum of valence band forever. We carry out the scattering phenomena by Monte Carlo method. two picture that be ladled by 'a1' and 'a2' refer to electrons and those one which be labeled by 'b1' and 'b2' refer to hole one. This pictures selected from thousand case for instance to show how electrons scattered to many level but the hole one dos not.
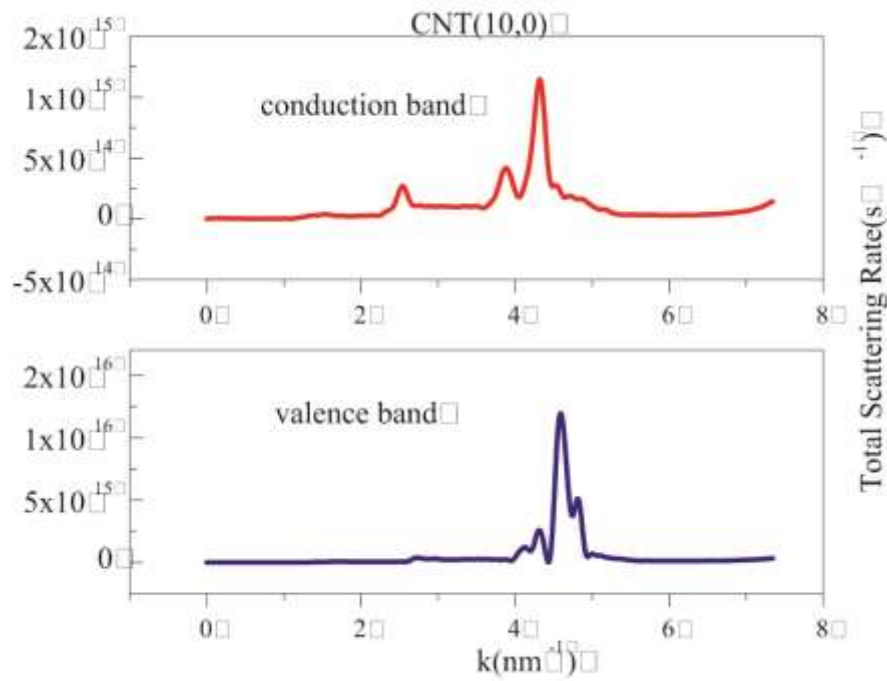
Figure   17:   This figure shows how electron scattered more than hole one. Electrons take a wide range of wave vector in scattering mechanism too but the hole one dose not.
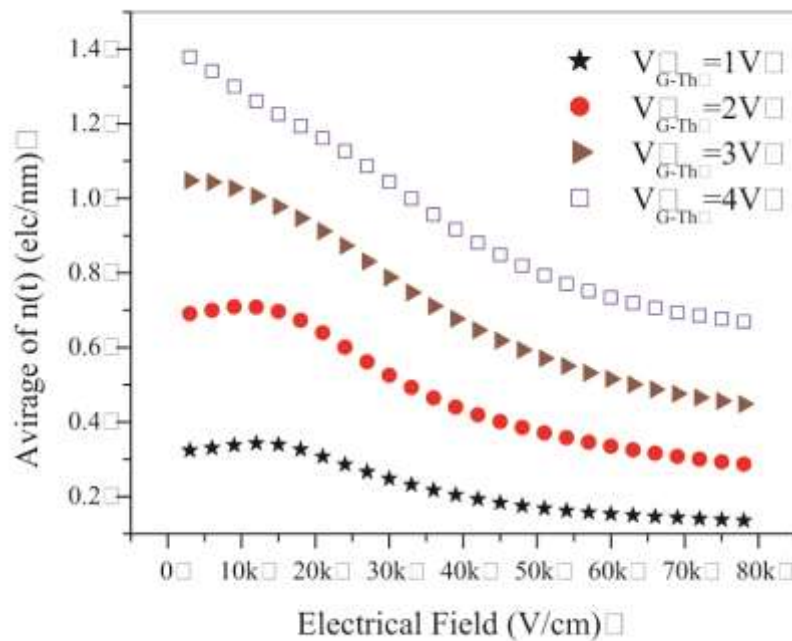
Figure   18:   This figure show the electron density in the CNT(10,0) (see Eq. 56, 57) for varus Gate voltage. When

we assume fermi level must be a fixed level it cause that some of free carrier be constrained in presence of electric field. The amount of this charge increase by increment on applied electric field.
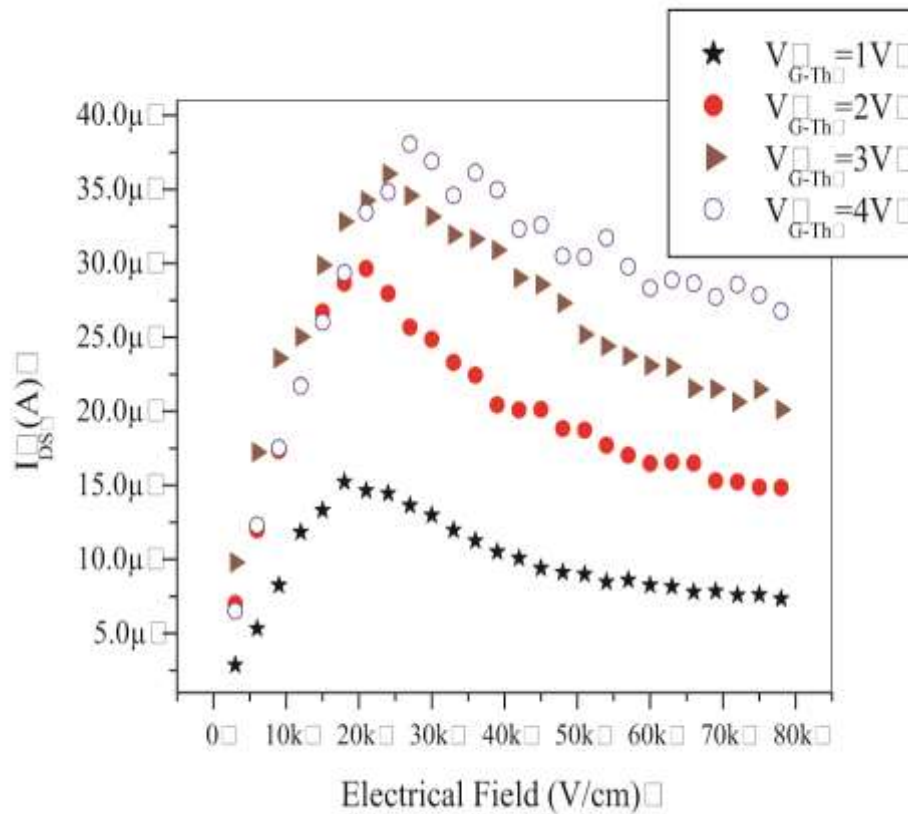

Figure   19:   This figure show the electron current from Source to Drain in a CNTFET which use a CNT(10,0) as it's channel. As you see the current has a maximum per the electric field which applied to its axis. When we increase the gate voltage the current which is transferred from Source to drain increase too.

REFERENCES

[1] Rodney S. Ruoff, Dong Qian, Wing Kam Liu, *C. R. Physique*, 4 (2003) 993–1008.

[2] Ph.Avouris, R.Martel, V.Derycke, J.Appenzeller, Physica B, 323 (2002) 6–14.

[3] Yiming Li, Hung-Mu Chou, Jam-Wem Lee, Bo-Shian Lee, *Microelectronic Engineering*, 81 (2005) 434–440.

[4] Anisur Rahman, Jing Guo, Supriyo Datta, Fellow, IEEE, and Mark S. Lundstrom, Fellow, IEEE, *IEEE TRANSACTIONS ON ELECTRON DEVICES*, 50 (2003) 1853-1864.

[5] A. Baharia, P. Morgena and Z.S. Lic, *Surface Science*, 602 (2008) 2315-2324.

[6] A. Bahari, U. Robenhagen, P. Morgen and Z. S. Li, *Phys. Rev. B*, 72 (2005) 205323.

[7] F. M. Nakhei and A. Bahari, *Int. J. Phys. Sci* , 4 (2009) 290-293.

[8] L. Marty, A . Iaia, M . Faucher, V. Bouchiat, C . Naud,M. Chaumont, T. Fournier, A.M. Bonnot, *Thin Solid Films*, 501 (2006) 299 – 302.

[9] Madhu Menon, Deepak Srivastava, *PHYSICAL REVIEW LETTERS*, 79 (1997) 4453-4456.

[10]   H. Rai-Tabar, *Physics Reports*, 390 (2004) 235–452.

[11]   Carbon Nanotubes, *Topics in Applied Physics* 80, ISBN: 3-540-41086-4, (2001).

[12]   Introduction To Solid State Physics, Charles Kittel, ISBN:0-471-11181-3.

[13] Michael J. Leamy, *International Journal of Solids and Structures*, 44 (2007) 874–894.

[14] Physical Properties of Carbon Nanotubes, R. Saito, G. Dresselhaus and M. S. Dresselhaus, ISBN: 1-86094-093-5, (1998).

[15]   Carbon Nanotubes Quantum Cylinders of Graphene, S. Saito and A. Zettl, ISBN: 978-0-444-53276-3, (2008).

[16] Neil W. Ashcroft, N. David Mermin, *Solid State Physics*, ISBN: 0-03-083993-9 (1976).

[17] G. S. Painter and D. E. Ellis, *Phys. Rev. B*, 1 (1970) 4747.

[18] R. A. Jishi, D. Inomata, K. Nakao, M. S. Dresselhaus, and G. Dresselhaus, *J.Phys.Soc.Jap.*, 63 no.6 (1994) 2252-2260,

[19]   W. Hoenlein, F. Kreupl, G.S. Duesberg, A.P. Graham, M. Liebau, R. Seidel, E. Unger, *Materials Science and Engineering C*, 23 (2003) 663 – 669.

[20] R. A. Jishi, D. Inomata, K. Nakao, M. S. Dresselhaus, and G. Dresselhaus, *J.Phys.Soc.Jap*, 63 (1994) 2252-2260 .

[21] R. A. Jishi, L. Venkataraman, M. S. Dresselhaus, and G. Dresselhaus, *Chem.Phys.Lett*, 209 (1993) 77-82.

[22] P. C. Eklunda, J. M. Holdena, and R. A. Jishi, *Carbon*, 33 (1995) 959-972.

[23] J. Yu, R. K. Kalia, and P. Vashishta, *J.Chem.Phys*, 103 (1995) 6697-6705.

[24] M. Menon, E. Richter, and K. R. Subbaswamy, *J.Chem.Phys*,104 (1995) 5875-5882.

[25] J. Kürti, G. Kresse, and H. Kuzmany, *Phys.Rev.B*, 58(1998) 8869-8872.

[26] O. Dubay and G. Kresse, *Phys.Rev.B*, 67 (2003) 035401

[27] V. N. Popov, V. E. V. Doren and M. Balkanski, *Phys.Rev.B*, 59, (1999) 8355-8358, .

[28] V. N. Popov and P. Lambin, *Phys.Rev.B*, 73 (2006) 085407.

[29] A. Bahari and M. Amiri, *ACTA PHYSICA POLONICA A* , 115 (2009) 625-628.

[30]   V. N. Popov, V. E. V. Doren and M. Balkanski, *Phys.Rev.B*, 59, (1999) 8355-8358.

[31]   A. Grouneis, R. Saito, T. Kimura, L. C. Cancado, M. A. Pimienta, A. Jorio, A. G. Souza Filho, G. Dresselhaus and M. S. Dresselhaus,   *Phys. Rev*, B65 (2002) 155405 .

[32] J.M. Leamy, *Int. J. Solids Struct*, 44 (2007) 874 .

[33] J. Che, T. Cagin, W. Go ddard, *Nanotechnology*, 10(1999) 263.

[34] J.-P.Ryckaert and A.Bellemans, *Faraday Discussions of the Chemical Society*, 66 (1978) 95-106 .

[35] D.V. Pozdnyakov, V.O. Galenchik, F.F. Komarov, V.M. Borzdov, *Physica E*, 33 (2006) 336 – 342.

[36] Zh. Yao, Ch.L. Kane, C. Dekker, *Phys. Rev. Lett.*, 84 (2000) 2941.

[37] Ali Javey, Hydoungsub Kim, Markus Brink, Qian Wang, Ant Ural, Jing Guo, Paul Mcintyre, Paul Mceuen, Mark Lundstrom and Hongjie Dai, *Nature materials*, 1 (2002) 241.

[38] Y.X.Liang,T.H.Wang, *Physica E*, 23 (2004) 232–236.

[39] G. Pennington and N. Goldsman, *Phys. Rev. B*, 68 (2003) 45426.

[40] G. Pennington and N. Goldsman, *IEICE Trans. Elect*, 86 (2003) 372

[41] Y. Xiaol, X. H. Yan, J. X. Cao and J.W. Ding, *J. Phys. Condens. Matter*, 15 (2003) L341.

[42] A. S. Davydov, *Quantum Mechanics*, ISBN: 0080204376, *Pergamon Pr* (1976).